prosthesis

MDPI

Case Report

Customized Facial Orthopedics: Proof of Concept for Generating 3D-Printed Extra-Oral Appliance for Early Intervention in Class III Malocclusion

Vincenzo Ronsivalle [1,*], Giorgio Gastaldi [2], Gianluigi Fiorillo [2], Alessandra Amato [3], Carla Loreto [4], Rosalia Leonardi [1] and Antonino Lo Giudice [1]

[1] Department of Medical-Surgical Specialties, School of Dentistry, University of Catania, Via Santa Sofia 78, 95123 Catania, Italy; rleonard@unict.it (R.L.); antonino.logiudice@unict.it (A.L.G.)
[2] Department of Dentistry, IRCCS San Raffaele Hospital, Dental School, Vita-Salute San Raffaele University, 20132 Milan, Italy; gastaldi.giorgio@unisr.it (G.G.); gianluigifiorillo@gmail.com (G.F.)
[3] Department of Neurosciences, Reproductive Sciences and Oral Sciences, University of Naples Federico II, Via Pansini 5, 80131 Naples, Italy; aale.amato@gmail.com
[4] Department of Biomedical and Biotechnology Sciences, Section of Human Anatomy, Histology and Sciences of Movement, University of Catania, 95123 Catania, Italy; carla.loreto@unict.it
* Correspondence: vincenzo.ronsivalle@hotmail.it

Abstract: Background: The present case report serves as a proof of concept for the fabrication and effective clinical administration of a 3D-printed chin cup tailored to the patient's anatomical characteristics. Methods: An 11-year-old male with a Class III malocclusion was treated using a chin cup appliance to intercept and control a Class III mandibular skeletal growing pattern early. Two tailored chin cup devices were designed using 3D face scanning and CBCT scanning and were produced with additive manufacturing techniques. The chin pads were digitally designed based on a 3D scan of the patient's face. The 3D modeling of chin cup components was performed using 3Shape Appliance Designer and 3D printed with biocompatible resin. An analogic chin pad was also produced for the same patient. The treatment plan involved the patient wearing the chin cup for 13 h per day. The patient was instructed to use all three chin pads produced at intervals of 4 months. The patient's experience was assessed by reporting the comfort experience via a VAS scale. The treatment strategy was effective in improving the skeletal Class III malocclusion. Additionally, the integration of 3D face scanning (or CBCT scanning), modeling, and printing enables the production of customized chin cups with superior fit and comfort, contributing to enhanced patient compliance and treatment efficacy.

Keywords: class III malocclusion; cad-cam; facial orthopedics

Citation: Ronsivalle, V.; Gastaldi, G.; Fiorillo, G.; Amato, A.; Loreto, C.; Leonardi, R.; Lo Giudice, A. Customized Facial Orthopedics: Proof of Concept for Generating 3D-Printed Extra-Oral Appliance for Early Intervention in Class III Malocclusion. *Prosthesis* **2024**, *6*, 135–145. https://doi.org/10.3390/prosthesis6010011

Academic Editors: Giuseppe Solarino and Roberto Sorrentino

Received: 11 December 2023
Revised: 26 January 2024
Accepted: 29 January 2024
Published: 1 February 2024

1. Introduction

Skeletal Class III malocclusion is a prevalent dental issue arising from either maxillary retrusion, mandibular protrusion, or a combination of both [1–3]. It often leads to complicated dentoalveolar issues, such as anterior edge-to-edge or anterior and/or posterior crossbite [4,5]. Class III malocclusion patients may have an unattractive concave profile, limited vertical function patterns, and potential aesthetic problems [3,4,6]. The prevalence of this malocclusion varies among populations [7,8] and is higher in Asian populations (23%) compared to Hispanics (9%), Caucasians (5%), and Africans (5%) [7,9–11]. The treatment of Class III malocclusion is often a challenge for orthodontists [9] and the concept of initiating early intervention is claimed to reduce the risk of significant orthodontic camouflage at the permanent dentition stage or surgical intervention [12].

Functional appliances, face masks, and chin cups (CCs) represent the treatment options featuring adequate scientific evidence [7]. In this regard, CCs are designed for the early orthopedic management of prognathic-growing patients [13–16]. Various studies have investigated their clinical effectiveness, indicating general improvement of Class III malocclusion through backward and downward mandibular rotation, retardation of mandibular growth, remodeling of the mandible and the temporomandibular joint (TMJ), retroclination of mandibular incisors, and closing of the gonial angle [9,10,13,15,17,18]. Currently, clinicians can use prefabricated CCs and customized CCs generated from chin impressions. Prefabricated CCs have some drawbacks due to inadequate adaptation that frequently leads to skin irritation and occasionally mild swelling during the application of the elastic traction, which can adversely impact patient compliance [19]. On the other hand, the customization process of CCs improves the appliance fitting and comfort by tailoring the shape and dimensions of the chin cup components to match the patient's anatomical characteristics. In fact, custom-made CCs are generated from the impression of the chin with alginate or polyvinyl-siloxane (PVS), thus limited to an analogic manufacturing process.

Nowadays, a three-dimensional (3D) representation of the patient's facial anatomy can be obtained through a completely non-invasive method using a facial scanner (FS) or Cone Beam computer tomography (CBCT). In this regard, the components of the chin cup could be designed and customized based on the patient's 3D facial reconstruction. For this purpose, specific 3D modeling software is needed, while the modeled components can be generated using additive manufacturing techniques (3D-printing technology). Although CBCT images provide a detailed three-dimensional definition of skeletal structures, some limitations have been documented in assessing soft tissues due to suboptimal resolution, substantial interslice intervals, lack of color representation, and extended scanning duration [20,21]. There are also ethical issues related to the radiation exposure of growing subjects, limiting the usage of CBCT only to specific clinical circumstances [22,23]. On the contrary, the facial scanning system enables the acquisition of high-resolution texture and color details of the facial region without introducing additional radiation risks. These advantages would support the employment of facial scan technology in clinical settings when facial soft-tissue assessment is necessary. Furthermore, this approach is accompanied by benefits like swift scanning duration, absence of ocular hazards, high reproducibility, and user-friendly operability [24].

With this notion in mind, the present case report describes a versatile digital workflow applied to generate a customized chin cup from CBCT or facial scan for the treatment of a child affected by Class III malocclusion. This case report was also supported by a digital analysis of the accuracy of the CBCT-based and FS-based customized chin cups in comparison with the actual gold standard manufacturing approach based on the analogical impression of the chin.

2. Materials and Methods

2.1. Clinical Examination

The present case report describes the treatment plan of an 11-year-old male referred for orthodontic consultation at the Department of Orthodontics of Catania University. In the frontal view, the patient exhibited facial symmetry, a significant increment of the lower face third, and no gingival exposure while smiling (Figure 1A,B).

Figure 1. Pre-treatment extra-oral examination: (**A**) Frontal view, (**B**) smiling frontal view, (**C**) lateral view.

In the lateral view, the facial profile was flat with a significant prominence of the chin, normal naso-labial angle and lip competence, and a remarkable downward and backward inclination of the mandible (Figure 1C). Intra-oral examination revealed a mild Class II molar and canine dental relationship in mixed dentition, deep bite, minimal overjet, and moderate lower crowding (Figure 2A–E).

Figure 2. Pre-treatment intra-oral examination. (**A**–**C**) Point of view (POV) of occlusion, (**D**) upper arch, (**E**) lower arch.

Cephalometric analysis revealed a skeletal class III discrepancy (ANB = −1.4ˆ) with increased mandibular body length (Go-Gn = 70.2 mm), severe negative value of facial convexity angle (Na-Apoˆ = −6.4ˆ), hyperdivergent mandibular vertical growth pattern (MP-SN = 31.9ˆ), and significant retro-inclination of the lower incisors (IMPAˆ = 80) (Figure 3A,B). Comparing intra-oral and cephalometric data, there was a remarkable inconsistency between dental malocclusion (Class II) and skeletal sagittal discrepancy (Class III) that could be attributed to the dental compensation of the malocclusion. The panoramic radiograph revealed a normal stage of tooth eruption and an absence of inflammatory conditions (Figure 4).

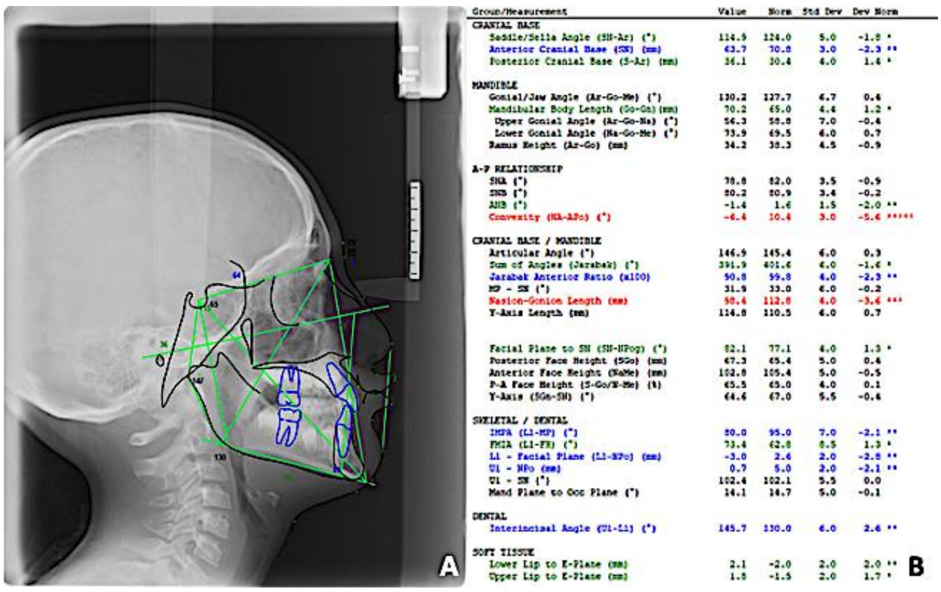

Group/Measurement	Value	Norm	Std Dev	Dev Norm
CRANIAL BASE				
Saddle/Sella Angle (SN-Ar) (°)	114.9	124.0	5.0	-1.8 *
Anterior Cranial Base (SN) (mm)	63.7	70.8	3.0	-2.3 **
Posterior Cranial Base (S-Ar) (mm)	36.1	30.4	4.0	1.4 *
MANDIBLE				
Gonial/Jaw Angle (Ar-Go-Me) (°)	130.2	127.7	6.7	0.4
Mandibular Body Length (Go-Gn) (mm)	70.2	65.0	4.4	1.2 *
Upper Gonial Angle (Ar-Go-Na) (°)	56.3	58.8	7.0	-0.4
Lower Gonial Angle (Na-Go-Me) (°)	73.9	69.5	6.0	0.7
Ramus Height (Ar-Go) (mm)	34.2	38.3	4.5	-0.9
A-P RELATIONSHIP				
SNA (°)	78.8	82.0	3.5	-0.9
SNB (°)	80.2	80.9	3.4	-0.2
ANB (°)	-1.4	1.6	1.5	-2.0 **
Convexity (NA-APo) (°)	-6.4	10.4	3.0	-5.6 *****
CRANIAL BASE / MANDIBLE				
Articular Angle (°)	146.9	145.4	6.0	0.3
Sum of Angles (Jarabak) (°)	391.9	401.6	6.0	-1.6 *
Jarabak Anterior Ratio (x100)	50.8	59.8	4.0	-2.3 **
MP - SN (°)	31.9	33.0	6.0	-0.2
Nasion-Gonion Length (mm)	98.4	112.8	4.0	-3.6 ***
Y-Axis Length (mm)	114.8	110.5	6.0	0.7
Facial Plane to SN (SN-NPog) (°)	82.1	77.1	4.0	1.3 *
Posterior Face Height (SGo) (mm)	67.3	65.4	5.0	0.4
Anterior Face Height (NaMe) (mm)	102.8	105.4	5.0	-0.5
P-A Face Height (S-Go/N-Me) (%)	65.5	65.0	4.0	0.1
Y-Axis (SGn-SN) (°)	64.6	67.0	5.5	-0.4
SKELETAL / DENTAL				
IMPA (L1-MP) (°)	80.0	95.0	7.0	-2.1 **
FMIA (L1-FH) (°)	73.4	62.8	8.5	1.3 *
L1 - Facial Plane (L1-NPo) (mm)	-3.0	2.6	2.0	-2.8 **
U1 - NPo (mm)	0.7	5.0	2.0	-2.1 **
U1 - SN (°)	102.4	102.1	5.5	0.0
Mand Plane to Occ Plane (°)	14.1	14.7	5.0	-0.1
DENTAL				
Interincisal Angle (U1-L1) (°)	145.7	130.0	6.0	2.6 **
SOFT TISSUE				
Lower Lip to E-Plane (mm)	2.1	-2.0	2.0	2.0 **
Upper Lip to E-Plane (mm)	1.8	-1.5	2.0	1.7 *

Figure 3. Pre-treatment cephalometric analysis. (**A**) Cephalometric tracing, (**B**) cephalometric parameters(°: angular measurements, mm: millimetric measurements, %: ratio).

The treatment plan involved the application of a chin cup appliance with the aim of improving the inter-jaw base relationship by controlling the sagittal and vertical growth of the mandible. Below is a detailed description of the analogical and digital workflow used to generate three chin cups for the same patient, an analogic-based chin cup, FS-based chin cup, and CBCT-based chin cup, respectively. The digital workflow used to evaluate the accuracy of all three appliances is also described.

Figure 4. Panoramic radiograph.

2.2. Customized Chin Cup Appliances

2.2.1. Analogic Workflow (Analogic-CC)

An analogical chin impression was taken to customize a third chin cup using a conventional analogical approach. The patient was initially placed in a seated position, and an elastomeric impression (Elite HD+, Zhermack, Badia Polesine, Italy) of the chin region was obtained. This was followed by the fabrication of a plaster model using Type IV plaster (Vel-Mix Stone, Kerr). Subsequently, on the plaster model, the chin cup was generated with 3 mm thick polylactic acid (PLA) thermoplastic material using a pressure form.

2.2.2. Stereolithography-Based Workflow (FS-CC)

For the stereolithographic digital workflow, preliminary 3D facial scanning was obtained with an OBI facial scanner (FifthIngenium, Milan, Italy). According to the previous literature [25], scanning was performed in a bright room and care was taken to keep the patient's hair away from the forehead and to avoid the projection of shadows on the face. The patient was asked to sit in a resting posture and to keep the teeth in occlusion and the lips relaxed. A robotic voice guided the child to tilt and rotate the head as needed for proper image capturing, which was completed within a few seconds (Figure 5A). The acquired 3D scan was then exported in .stl format. The .stl file reproducing facial soft tissues was imported into the 3Shape Appliance Designer (3Shape, Copenhagen, Denmark) software; the customized chin cup on the facial scan was modeled with a thickness of 3 mm and afterward, it was exported in .stl file format (Figure 5B,C). Therefore, the generated chin cup was 3D-printed using BioMed White Resin (Formlab, Somerville, MA, USA) and Form 3B printers (Formlab, Somerville, MA, USA). The 3D-printing setup was performed on the PreForm slicing software (Formlab, Somerville, MA, USA) with layer thickness set at 50 µm. The post-printing procedures were carried out as follows: two separate immersion baths of 97% isopropyl alcohol (Faichim, San Giovanni Lupatoto—VR, Italy) using the ultrasonic cleaner Eurosonic®3D (Euronda Spa, Sandrigo—VI, Italy), air drying at room temperature for 30 s, and one curing cycle of 15 min. The curing process was carried out using the Form Cure machine (wavelength 385–405 nm; Formlab, Somerville, MA, USA),

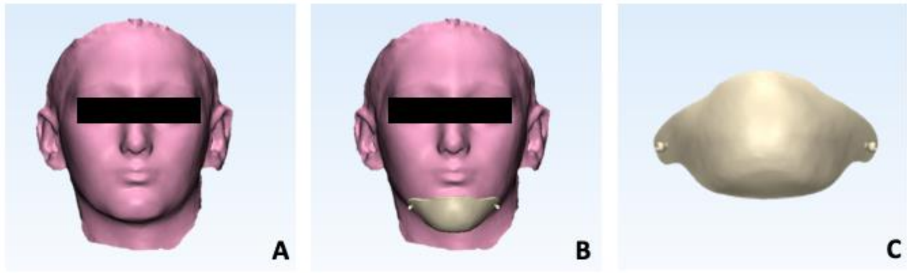

Figure 5. Stereolithography-based CC. (**A**) Facial scan, (**B**) prototype of CC, (**C**) digital CC.

2.2.3. CBCT-Based Workflow (CBCT-CC)

Since the patient required CBCT acquisition for oro-facial surgery evaluation, we had the possibility to use CBCT acquisition to generate a second CBCT-based chin cup for the same patient. A CBCT scan was conducted using ICAT (Imaging Sciences International, Hartfield, PA, USA) and subsequently converted into a Digital Imaging and Communications in Medicine (DICOM) file. The scanning protocol employed featured isotropic voxels measuring 0.3 mm in size, an acquisition time of 8.9 s, a wide field of view of 120 kV, and a current of 20 mA. Subsequently, utilizing Mimics 21.0 software (Materialise, Leuven, Belgium), the segmentation of the facial soft tissue was executed, and the resulting data were exported in .stl file format (Figure 6A). This 3D model of the facial soft tissue was imported into the 3Shape Appliance Designer software for the purpose of designing a customized chin cup with a thickness of 3 mm (Figure 6B,C). The designed chin cup was subsequently generated through 3D printing, using the same materials and settings as the FS-CC.

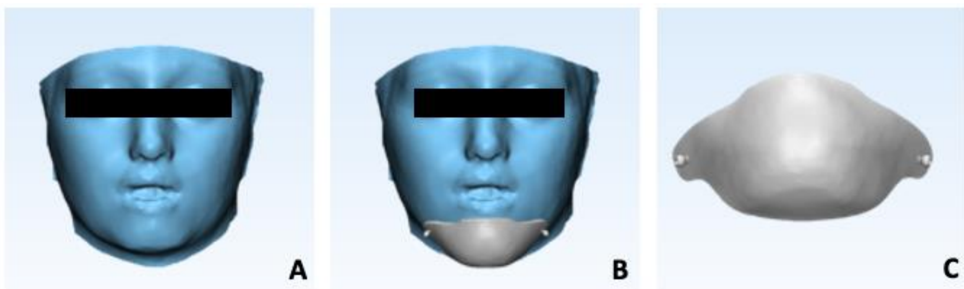

Figure 6. CBCT-based CC. (**A**) Facial scan, (**B**) prototype of CC, (**c**) digital CC.

The three generated CCs were finally scanned using the 3Shape E1 (3Shape, Copenhagen, Denmark) laboratory scanner, featuring a scanning resolution of 10 µm. The generated digital models of the chin cups were exported as .stl files to perform subsequent analysis of accuracy.

2.3. Treatment Plan

The patient was asked to wear the chin cup at least for 14 h per day and was monitored at monthly scheduled appointments to verify compliance and manage potential appliance side effects such as soft tissue irritation. The patient was also asked to use all three chin cups generated for 4 months each and to provide comfort data using the VAS scale at the end of the wearing period. Concerning the treatment plan chosen, the parents were informed that a second treatment stage involving a fixed appliance would be considered only after the end of facial growth since at this age it is not possible to exclude the necessity of orthognathic surgery in adulthood.

2.4. Superimposition, Matching Percentage Calculation, and Deviation Analysis

To perform a comparative analysis of the chin cups, it was imperative to establish alignment among them. To achieve this, an initial alignment was carried out by registering all chin cups with the model from which they were originally derived. For the analog model, this involved scanning the plaster chin model using the laboratory scanner (3Shape E1) and subsequently repeating the scan with the attached chin cup. Subsequently, both sets of data were imported in .stl format into 3-Matic software (Materialise, Leuven, Belgium). In the case of the models derived from the facial scan and CBCT, a similar alignment process was undertaken within the 3-Matic software. Specifically, the models of the chin cups, which had been scanned with the laboratory scanner, were aligned with the designed chin cups to ensure they shared a common chin coordinate system. For the purpose of comparison, the 3D soft tissue model obtained from the CBCT, the facial scan data, and the 3D plaster model of the chin were initially superimposed. This superimposition was achieved by first aligning them based on randomly selected points and subsequently refining the alignment using a best-fit algorithm. Afterward, using the "moving along entities" feature, the analogic CC, FS-CC, and CBCT-CC were placed in the same coordinate system and superimposed. It should be mentioned that the gold standard (GS) for this comparison research was the 3D analog chin cup model. The STL files of the superimposed chin cup models were imported into Geomagic Control X software (3D Systems, version 2018.1.1, 3D Systems, Rock Hill, SC, USA) to perform the deviation analysis. The software automatically calculates the mean and maximum values of the linear distances (Euclidean distance) between a GS and the other chin cup with different workflows. The range of tolerance was set to ±0.5 (0.03 mm) mm and this value was measured across 100% of the surface points and represented on a color map of the chin cup model, which showed the deviation in different colors. When the distance values were greater than the positive limits of the ranges of tolerance, they were represented in red, whereas values smaller than the negative limits were represented in blue. Additionally, all the values included in the tolerance range were represented in green. Once the deviation analysis was carried out, the matching percentages (%) of all the distance values were calculated. These values represented the degree of matching between the two models and, thus, showed the accuracy between the GS and chin cups with different workflows (Figure 7).

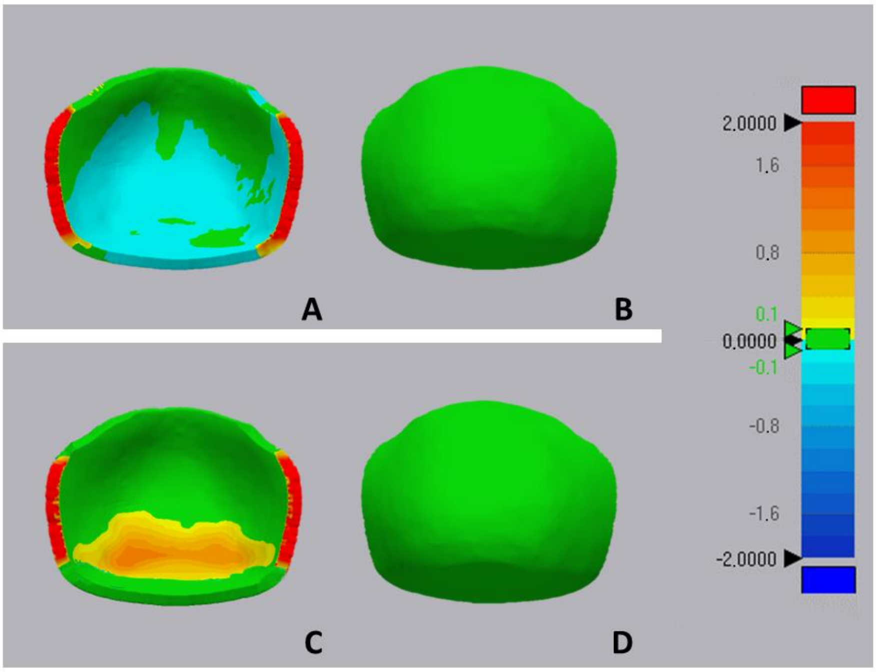

Figure 7. Deviation analysis. (**A**) Frontal view of stereolithography-based CC, (**B**) posterior view stereolithography-based CC, (**C**) frontal view of CBCT-based CC, (**D**) posterior view of CBCT-based CC.

3. Results

3.1. Clinical Outcomes

Twelve months after treatment, the patient underwent an orthodontic diagnostic check-up to verify treatment progress. As expected, the patient maintained baseline facial characteristics related to the facial growth pattern (Figure 8A–C). The patient maintained the same slight Class II molar and canine dental relationship in mixed dentition. In general, intra-oral examination revealed a similar occlusal condition compared to the baseline except for the retro-inclination of the lower incisors (Figure 9A–E). Cephalometric analysis confirmed a significant improvement in skeletal parameters. In particular, the patient presented a normal sagittal skeletal relationship (ANBˆ = 1.8) with a significant improvement in the facial convexity angle (Na-Apoˆ = −0.6) and a hyperdivergent mandibular vertical growth pattern (MP-SN = 31.6ˆ); however, there was a significant retro-inclination of the lower incisors (IMPAˆ = 76.1) that should be interpreted as the consequence of the application of distal forces generated in the anterior mandibular region (Figure 10A,B). At this stage, the patient was asked to reduce wearing time and to wear the appliance only at night.

Figure 8. Post-treatment extra-oral examination. (**A**) Frontal view, (**B**) smiling frontal view, (**C**) lateral view.

Figure 9. Post-treatment intra-oral examination. (**A**–**C**) Point of view (POV) of occlusion, (**D**) upper arch, (**E**) lower arch.

The patient reported similar values of comfort with both FS-based and CBCT-based chin cups: 6.8 and 6.9 on the VAS scale, respectively. These values were also close to those reported with the analogic-based chin cup (5.3).

3.2. Deviation Analysis

According to the color map and the range of tolerance selected, the chin cups produced by digital workflows, the FS-based and CBCT-based chin cups, showed no relevant surface differences compared to the analogic-based chin cup, which represented the actual gold standard. Accordingly, both digital workflows provided an accurate definition of the chin cup clinically comparable with that obtained with analogic impression.

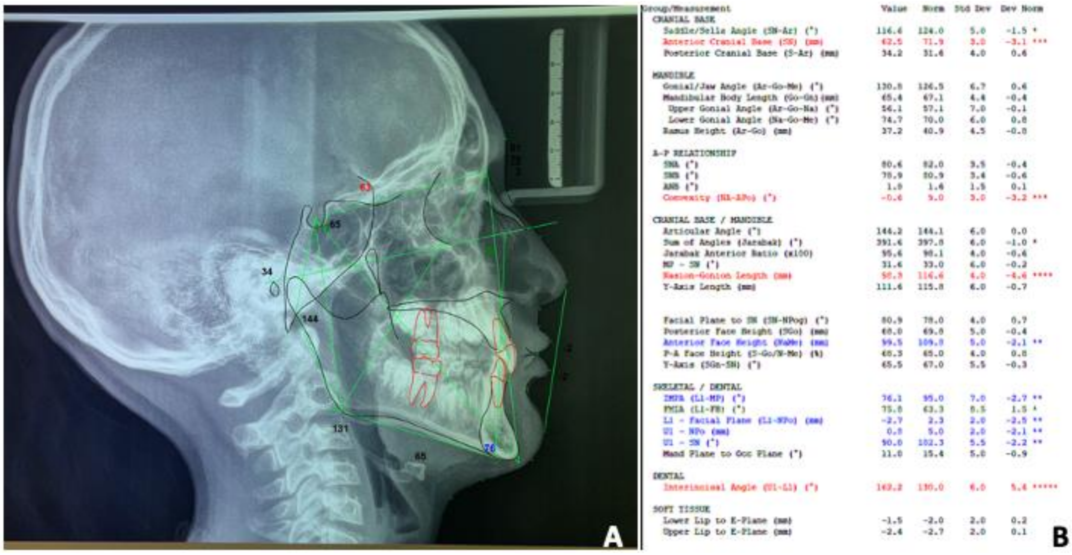

Group/Measurement	Value	Norm	Std Dev	Dev Norm
CRANIAL BASE				
Saddle/Sella Angle (SN-Ar) (°)	116.4	124.0	5.0	-1.5 *
Anterior Cranial Base (SN) (mm)	62.5	71.9	3.0	-3.1 ***
Posterior Cranial Base (S-Ar) (mm)	34.2	31.6	4.0	0.6
MANDIBLE				
Gonial/Jaw Angle (Ar-Go-Me) (°)	130.8	126.5	6.7	0.6
Mandibular Body Length (Go-Gn) (mm)	65.4	67.1	4.4	-0.4
Upper Gonial Angle (Ar-Go-Na) (°)	56.1	57.1	7.0	-0.1
Lower Gonial Angle (Na-Go-Me) (°)	74.7	70.0	6.0	0.8
Ramus Height (Ar-Go) (mm)	37.2	40.9	4.5	-0.8
A-P RELATIONSHIP				
SNA (°)	80.6	82.0	3.5	-0.4
SNB (°)	78.9	80.9	3.4	-0.6
ANB (°)	1.8	1.6	1.5	0.1
Convexity (NA-APo) (°)	-0.6	9.0	3.0	-3.2 ***
CRANIAL BASE / MANDIBLE				
Articular Angle (°)	144.2	144.1	6.0	0.0
Sum of Angles (Jarabak) (°)	391.6	397.8	6.0	-1.0 *
Jarabak Anterior Ratio (x100)	95.6	98.1	4.0	-0.6
MP - SN (°)	31.6	33.0	6.0	-0.2
Nasion-Gonion Length (mm)	98.3	116.6	4.0	-4.6 ****
Y-Axis Length (mm)	111.6	115.8	6.0	-0.7
Facial Plane to SN (SN-NPog) (°)	80.9	78.0	4.0	0.7
Posterior Face Height (SGo) (mm)	68.0	69.8	5.0	-0.4
Anterior Face Height (NaMe) (mm)	99.5	109.8	5.0	-2.1 **
P-A Face Height (S-Go/N-Me) (%)	68.3	65.0	4.0	0.8
Y-Axis (SGn-SN) (°)	65.5	67.0	5.5	-0.3
SKELETAL / DENTAL				
IMPA (L1-MP) (°)	76.1	95.0	7.0	-2.7 **
FMIA (L1-FH) (°)	75.8	63.3	8.5	1.5 *
L1 - Facial Plane (L1-NPo) (mm)	-2.7	2.3	2.0	-2.5 **
U1 - NPo (mm)	0.8	5.0	2.0	-2.1 **
U1 - SN (°)	90.0	102.3	5.5	-2.2 **
Mand Plane to Occ Plane (°)	11.0	15.4	5.0	-0.9
DENTAL				
Interincisal Angle (U1-L1) (°)	162.2	130.0	6.0	5.4 *****
SOFT TISSUE				
Lower Lip to E-Plane (mm)	-1.5	-2.0	2.0	0.2
Upper Lip to E-Plane (mm)	-2.4	-2.7	2.0	0.1

Figure 10. Post-treatment cephalometric analysis. (**A**) Cephalometric tracing, (**B**) cephalometric parameters(°: angular measurements, mm: millimetric measurements, %: ratio).

4. Discussion

Orthodontic/dento-facial extra-oral appliances have always raised skepticism among young patients and parents; also, they are associated with negative feedback from parents and patients particularly related to the lack of stability and the experience of pain [26–28]. Since the extra-oral appliances available on the market are preformed, or at least available in a few different sizes/dimensions, they cannot be adapted to all patients due to facial variability among individuals. For this reason, patients often report that extra-oral appliances do not fit well or generate instability and asymmetric tension of the elastic traction [29]. This is particularly relevant in Class III subjects where a stable and firm chin pad is required to optimize the biomechanics of the applied forces and the patient's comfort, either when face mask or chin cup appliances are used. Indeed, non-customized pads could hit and hurt the skin of the chin since uncontrolled movements occur during the application of elastic force due to the absence of primary stability related to the consistency between appliance design and morphology of the chin. A recent well-conducted case report study focused on this topic and proposed a digital workflow to produce a customized 3D-printed face mask [26]. With this notion in mind, the presented case report serves as a proof of concept for the fabrication and effective clinical administration of a 3D-printed chin cup tailored to the patient's anatomical characteristics. This advancement is achieved through the utilization of innovative technologies such as non-invasive face scanning for 3D image acquisition, digital design, and additive manufacturing. Despite limitations, 3D facial scanners are valuable tools in dentistry due to their speed and non-invasiveness. They aid in various aspects of dental care, including interdisciplinary communication, smile design, and obstructive sleep apnea diagnosis. Additionally, they hold promise for future applications in craniofacial research and prosthodontic treatment planning [30]. Also, in 2019, Lavorgna et al.'s [31] study emphasized that photogrammetric scanners, in general, may have a smaller shooting field size and improved accuracy. Notwithstanding these factors, the photogrammetric facial scanner demonstrated outstanding performance in measuring small-sized face structures, indicating its broad versatility across various applications. The individualized chin cup garnered positive feedback from the patient and was effective in obtaining clinical outcomes. As opposed to face masks, the chin pad of CCs can be customized with analogical impressions; however, there are some clinical advantages of the proposed digital workflow that the authors summarized below. Recently, Reddy N. et al. [32] published a work about digital dentistry that clearly demonstrated how in an experimental laboratory environment, the utilization of digital methodologies does not substantially affect the precision of prosthesis construction when compared to traditional techniques.

Digital production and customization. Once a chin pad is designed using dedicated software, an open .stl file is produced and can be easily shared with the lab technician for final prototyping, even in case of future breakage of the appliance. Furthermore, it is possible to integrate digital fabrication tools to develop a range of colors and iconographic datasets that can be individualized for each patient, improving their acceptance of the appliance.

Comfort. Although the chin pad can be customized even with analogical impressions, the polylactic acid (PLA) material is heavier than the 3D-printed photopolymer resin used for appliance fabrications. Thus, subjects using conventional chin cups may experience more comfort using chin pads obtained from additive manufacturing. In this regard, the patient in the present case report reported better comfort with both 3D-printed FS-based and CBCT-based pads compared to the analogic pad.

Cost. Conventional chin cups are an expensive appliance since the clinician should purchase the headpiece, the elastic modules, and the security modules. Furthermore, the cost of the chin pad must be added since this part is completely designed and produced by the lab technician. With the digital workflow, it is possible to produce chin pads in-office with a significant reduction in overall costs.

5. Conclusions

The present case report proposes a proof of concept for the fabrication of a 3D-printed CC tailored to the patient's anatomical characteristics. For this purpose, we used a specific workflow to generate two 3D-printed chin pads obtained from FS and CBCT acquisitions, respectively. An analogic chin pad was also produced as the gold standard and both clinical data (comfort assessed via the VAS scale) and digital data (deviation analysis) were used to evaluate the appropriateness of FS-based and CBCT-based chin cups compared to analogic chin cups.

Both FS-based and CBCT-based chin cups were accurate and showed greater comfort reported by the patient compared to the analogic-based chin cup. Further studies are warmly encouraged to comparatively evaluate the long-term effectiveness and side effects related to the usage of analogic or 3D-printed chin cups. Another topic of interest would be the application of Artificial Intelligence in supporting the design and prototyping process of customized facial appliances [23].

Author Contributions: Conceptualization, G.G. and G.F.; methodology, V.R. and A.L.G.; software, V.R.; validation, C.L.; formal analysis, R.L.; investigation, V.R. and A.L.G.; data curation, A.A.; writing—original draft preparation, V.R.; writing—review and editing, A.L.G. All authors have read and agreed to the published version of the manuscript.

Funding: This research received no external funding.

Institutional Review Board Statement: The study was conducted in accordance with the Declaration of Helsinki and approved by the Institutional Review Board of the University of Catania (A.Q.A.M.DI. n. protocol 119/2020/PO) for studies involving humans.

Informed Consent Statement: Informed consent was obtained from all subjects involved in the study.

Data Availability Statement: The data presented in this study are available on request from the corresponding author.

Conflicts of Interest: The authors declare no conflicts of interest.

References

1. Sanborn, R.T.J.A.O. Differences between the Facial Skeletal Patterns of Class III Malocclusion and Normal Occlusion. *Angle Orthod.* **2009**, *25*, 208–222.
2. Guyer, E.C.; Ellis, E.E., 3rd; McNamara, J.A., Jr.; Behrents, R.G. Components of class III malocclusion in juveniles and adolescents. *Angle Orthod.* **1986**, *56*, 7–30. [CrossRef] [PubMed]

3. Williams, S.; Andersen, C.E. The morphology of the potential Class III skeletal pattern in the growing child. *Am. J. Orthod.* **1986**, *89*, 302–311. [CrossRef]
4. Karakıs, D.; Kaymak, D.; Dogan, A. The evaluation of maximum bite force in the occlusal rehabilitation of patient with Angle Class III malocclusion: A case report. *J. Adv. Prosthodont.* **2013**, *5*, 364–368. [CrossRef]
5. Ha, S.W.; Kim, S.J.; Choi, J.Y.; Baek, S.H. Characterization of facial asymmetry phenotypes in adult patients with skeletal Class III malocclusion using three-dimensional computed tomography and cluster analysis. *Korean J. Orthod.* **2022**, *52*, 85–101. [CrossRef]
6. Almokri, N.M.; Alsaggaf, D.H.; Alsulaimani, F.F.; Zawawi, K.H. Anthropometric and Cephalometric Facial Characteristics of Adult Saudi Patients with Skeletal Class III Malocclusions. *Contemp. Clin. Dent.* **2023**, *14*, 232–238. [CrossRef]
7. Hardy, D. Prevalence of angle class III malocclusion: A systematic review and meta-analysis. *Open J. Epidemiol.* **2012**, *2*, 75–82. [CrossRef]
8. Soh, J.; Sandham, A.; Chan, Y.H. Occlusal status in Asian male adults: Prevalence and ethnic variation. *Angle Orthod.* **2005**, *75*, 814–820. [CrossRef] [PubMed]
9. Toffol, L.D.; Pavoni, C.; Baccetti, T.; Franchi, L.; Cozza, P. Orthopedic treatment outcomes in Class III malocclusion. A systematic review. *Angle Orthod.* **2008**, *78*, 561–573. [CrossRef] [PubMed]
10. Zurfluh, M.A.; Kloukos, D.; Patcas, R.; Eliades, T. Effect of chin-cup treatment on the temporomandibular joint: A systematic review. *Eur. J. Orthod.* **2015**, *37*, 314–324. [CrossRef] [PubMed]
11. Silva, R.G.; Kang, D.S. Prevalence of malocclusion among Latino adolescents. *Am. J. Orthod. Dentofac. Orthop.* **2001**, *119*, 313–315. [CrossRef]
12. Proffit, W.R.; Fields, H.W.; Sarver, D.M. *Contemporary Orthodontics*; Mosby Elsevier: Philadelphia, PA, USA, 2007.
13. Liu, Z.P.; Li, C.J.; Hu, H.K.; Chen, J.W.; Li, F.; Zou, S.J. Efficacy of short-term chincup therapy for mandibular growth retardation in Class III malocclusion. *Angle Orthod.* **2011**, *81*, 162–168. [CrossRef] [PubMed]
14. Ritucci, R.; Nanda, R. The effect of chin cup therapy on the growth and development of the cranial base and midface. *Am. J. Orthod. Dentofac. Orthop.* **1986**, *90*, 475–483. [CrossRef]
15. De Clerck, H.J.; Proffit, W.R. Growth modification of the face: A current perspective with emphasis on Class III treatment. *Am. J. Orthod. Dentofac. Orthop.* **2015**, *148*, 37–46. [CrossRef]
16. Fiori, A.; Minervini, G.; Nucci, L.; d'Apuzzo, F.; Perillo, L.; Grassia, V. Predictability of crowding resolution in clear aligner treatment. *Prog. Orthod.* **2022**, *23*, 43. [CrossRef] [PubMed]
17. Chatzoudi, M.I.; Ioannidou-Marathiotou, I.; Papadopoulos, M.A. Clinical effectiveness of chin cup treatment for the management of Class III malocclusion in pre-pubertal patients: A systematic review and meta-analysis. *Prog. Orthod.* **2014**, *15*, 62. [CrossRef] [PubMed]
18. Minervini, G.; Del Mondo, D.; Russo, D.; Cervino, G.; D'Amico, C.; Fiorillo, L. Stem Cells in Temporomandibular Joint Engineering: State of Art and Future Persectives. *J. Craniofac. Surg.* **2022**, *33*, 2181–2187. [CrossRef]
19. Cacciatore, G.; Poletti, L.; Huanca Ghislanzoni, L. A chairside customized chin-cup. *J. Clin. Orthod. JCO* **2013**, *2013*, 352.
20. Ayoub, A.F.; Xiao, Y.; Khambay, B.; Siebert, J.P.; Hadley, D. Towards building a photo-realistic virtual human face for craniomaxillofacial diagnosis and treatment planning. *Int. J. Oral. Maxillofac. Surg.* **2007**, *36*, 423–428. [CrossRef]
21. Miracle, A.C.; Mukherji, S.K. Conebeam CT of the head and neck, part 1: Physical principles. *AJNR. Am. J. Neuroradiol.* **2009**, *30*, 1088–1095. [CrossRef]
22. Leonardi, R.M.; Aboulazm, K.; Giudice, A.L.; Ronsivalle, V.; D'Antò, V.; Lagravère, M.; Isola, G. Evaluation of mandibular changes after rapid maxillary expansion: A CBCT study in youngsters with unilateral posterior crossbite using a surface-to-surface matching technique. *Clin. Oral. Investig.* **2021**, *25*, 1775–1785. [CrossRef] [PubMed]
23. Lo Giudice, A.; Ronsivalle, V.; Gastaldi, G.; Leonardi, R. Assessment of the accuracy of imaging software for 3D rendering of the upper airway, usable in orthodontic and craniofacial clinical settings. *Prog. Orthod.* **2022**, *23*, 22. [CrossRef] [PubMed]
24. Ma, L.; Xu, T.; Lin, J. Validation of a three-dimensional facial scanning system based on structured light techniques. *Comput. Methods Programs Biomed.* **2009**, *94*, 290–298. [CrossRef] [PubMed]
25. Blasi, A.; Nucera, R.; Ronsivalle, V.; Candida, E.; Grippaudo, C. Asymmetry index for the photogrammetric assessment of facial asymmetry. *Am. J. Orthod. Dentofac. Orthop.* **2022**, *162*, 394–402. [CrossRef]
26. Franchi, L.; Vichi, A.; Marti, P.; Lampus, F.; Guercio, S.; Recupero, A.; Giuntini, V.; Goracci, C. 3D Printed Customized Facemask for Maxillary Protraction in the Early Treatment of a Class III Malocclusion: Proof-of-Concept Clinical Case. *Materials* **2022**, *15*, 3747. [CrossRef] [PubMed]
27. Kim, H.; Kim, J.S.; Kim, C.S.; Becker-Weimann, S.Y.; Cha, J.Y.; Choi, S.H. Skin irritation in children undergoing orthodontic facemask therapy. *Sci. Rep.* **2023**, *13*, 2200. [CrossRef] [PubMed]
28. Kwak, H.J.; Park, H.J.; Kim, Y.J.; Lee, D.Y. Factors associated with long-term vertical skeletal changes induced by facemask therapy in patients with Class III malocclusion. *Angle Orthod.* **2018**, *88*, 157–162. [CrossRef] [PubMed]
29. Arreghini, A.; Trigila, S.; Lombardo, L.; Siciliani, G. Objective assessment of compliance with intra- and extraoral removable appliances. *Angle Orthod.* **2017**, *87*, 88–95. [CrossRef]
30. Lee, J.D.; Nguyen, O.; Lin, Y.-C.; Luu, D.; Kim, S.; Amini, A.; Lee, S.J. Facial Scanners in Dentistry: An Overview. *Prosthesis* **2022**, *4*, 664–678.

31. Lavorgna, L.; Cervino, G.; Fiorillo, L.; Di Leo, G.; Troiano, G.; Ortensi, M.; Galantucci, L.; Cicciù, M. Reliability of a Virtual Prosthodontic Project Realized through a 2D and 3D Photographic Acquisition: An Experimental Study on the Accuracy of Different Digital Systems. *Int. J. Environ. Res. Public Health* **2019**, *16*, 5139. [CrossRef]
32. Reddy, N.; Vempalli, S.; Prakash, J.; Suganna, M.; Meenakshi, S.I.; Shivakumar, G.C.; Crimi, S.; Minervini, G. Evaluation of the Effect of Digital Dentistry on the Accuracy of Implant Placement and Prosthesis Fabrication— A Systematic Review and Meta-Analysis. *Prosthesis* **2023**, *5*, 666–677.